TRIM21 mediates antibody inhibition of adenovirus-based gene delivery and vaccination

Maria Bottermann[a], Stian Foss[b,c,d], Laurens M. van Tienen[a], Marina Vaysburd[a], James Cruickshank[a], Kevin O'Connell[a], Jessica Clark[a], Keith Mayes[a], Katie Higginson[a], Jack C. Hirst[e], Martin B. McAdam[c], Greg Slodkowicz[a], Edward Hutchinson[e], Patrycja Kozik[a], Jan Terje Andersen[b,c,d], and Leo C. James[a,1]

[a]Protein and Nucleic Acid Chemistry Division, Medical Research Council, Laboratory of Molecular Biology, Cambridge CB2 0QH, United Kingdom; [b]Department of Biosciences, Centre for Immune Regulation, University of Oslo, N-0316 Oslo, Norway; [c]Department of Immunology, Centre for Immune Regulation, Oslo University Hospital, N-0372 Oslo, Norway; [d]Department of Pharmacology, Institute of Clinical Medicine, University of Oslo, N-0372 Oslo, Norway; and [e]MRC-University of Glasgow Centre for Virus Research, Glasgow G61 1QH, United Kingdom

Adenovirus has enormous potential as a gene-therapy vector, but preexisting immunity limits its widespread application. What is responsible for this immune block is unclear because antibodies potently inhibit transgene expression without impeding gene transfer into target cells. Here we show that antibody prevention of adenoviral gene delivery in vivo is mediated by the cytosolic antibody receptor TRIM21. Genetic KO of TRIM21 or a single-antibody point mutation is sufficient to restore transgene expression to near-naïve immune levels. TRIM21 is also responsible for blocking cytotoxic T cell induction by vaccine vectors, preventing a protective response against subsequent influenza infection and an engrafted tumor. Furthermore, adenoviral preexisting immunity can lead to an augmented immune response upon i.v. administration of the vector. Transcriptomic analysis of vector-transduced tissue reveals that TRIM21 is responsible for the specific up-regulation of hundreds of immune genes, the majority of which are components of the intrinsic or innate response. Together, these data define a major mechanism underlying the preimmune block to adenovirus gene therapy and demonstrate that TRIM21 efficiently blocks gene delivery in vivo while simultaneously inducing a rapid program of immune transcription.

TRIM21 | adenovirus | host–pathogen | gene therapy | viral vector

Adenoviral vectors are the most frequently used delivery vehicles in gene therapy clinical trials (1) and have enormous potential as vaccine vectors and oncolytic agents in cancer treatment (2). They are attractive because they can be grown to high titers, their genome sequence can easily be manipulated, and they induce robust transgene expression in a variety of dividing and nondividing cell types. Despite these advantageous properties, the high level of preexisting immunity in the human population prevents their widespread use. This is particularly true for adenovirus 5 (Ad5) (3–5), the subtype on which most adenoviral vectors have been based. Preexisting humoral immunity is a correlate of poor transgene expression (6) and, during vaccination, a subsequently diminished CD8 T cell response against the desired antigen (6–9). Therefore, knowing what mediates the block to transgene expression and activates the immune response in the presence of anti-Ad5 antibodies might provide insight into new approaches to circumvent preexisting immunity. The majority of anti-Ad5 neutralizing Abs (NAbs) are directed against the major coat protein hexon (5, 10, 11), and more specifically its solvent-exposed hypervariable regions (HVRs) (12). As hexon is not involved in the coxsackie and adenovirus receptor (CAR)-dependent entry mechanism that Ad5 uses, which is mediated by fiber and penton base (13, 14), the neutralizing effect is unlikely to involve classical entry blocking.

We have previously shown that the cytosolic antibody receptor TRIM21 mediates the efficient cytosolic neutralization of antibody-bound Ad5 in vitro. Ad5 gains access to the cytosol during infection through penetration of early endosomes shortly after endocytosis and can therefore carry antibody into the cytosol. Upon binding to the Fc region of IgG with its PRYSPRY

motif, TRIM21 becomes activated and sequentially recruits the E2 enzymes Ube2W and Ube2N/Ube2V2, which N-terminally polyubiquitinate TRIM21 with anchored K63 chains. This results in recruitment of the proteasome and rapid degradation of the viral particle while, simultaneously, the proteasome-associated deubiquitinase PohI liberates the K63-linked ubiquitin chains, which stimulate innate immune signaling pathways (15–18). Furthermore, degradation of the viral capsid results in the exposure of the Ad5 DNA to the cytosolic DNA sensor cGAS, which can initiate a second wave of innate immune signaling (19).

Here we investigate what role TRIM21 has in the preexisting immune block to Ad5 gene delivery in vivo and in the activation of innate immune signaling.

Results

As hexon is the immunodominant antigen in preexisting Ad5 immunity, we chose as a model the anti-hexon mouse–human chimeric IgG1 monoclonal antibody (mAb) 9C12 (rh9C12), which binds two of the hexon HVRs (20). First, we investigated

Significance

Viral-based delivery vectors have huge potential in the treatment of human disease. Adenoviral vectors specifically have proven highly efficacious in delivering corrected genes, as part of gene therapy, and vaccine epitopes for treating cancer and infectious disease. A principal obstacle to their widespread use is that antibodies potently neutralize them, limiting treatment to naïve patients. How antibodies block adenovirus-based transduction has long remained a mystery because, even though they prevent transgene expression, they do not prevent transgene delivery into target tissue. Here we show that the cytosolic antibody receptor TRIM21 is responsible for intercepting adenoviral gene therapy and vaccine vectors and neutralizing them. Gene KO of TRIM21 or a single-antibody mutation that prevents interaction is sufficient to restore transgene expression.

whether vector uptake in vivo was inhibited by rh9C12 via a receptor-blocking effect. Mice were injected with rh9C12 2–4 h before injection with Ad5 to mimic circulating humoral immunity to the virus. Livers were harvested 2–8 h postinfection, and quantitative PCR (qPCR) was used to quantify viral genomes within the tissue. At no time point did we observe a difference in genome delivery in the presence of antibody (Fig. 1A). To assess whether rh9C12 diminishes transgene expression, we looked at liver transduction by Ad5 carrying the luciferase gene (Ad5-Luc) and found that, although rh9C12 did not affect viral gene transfer, it diminished transgene expression 1,000-fold (Fig. 1C). A possible explanation for this observed discrepancy is that the presence of antibody alters transgene expression by changing the entry route of virus into cells and preventing access to the cytosol. Antibody has previously been shown to allow uptake by

liver-resident Kupffer cells by engaging FcγRs (21), which might result in decreased infection. We produced a "LALA" (L234A/L235A) mutant of rh9C12, which significantly diminishes FcγR binding by ablating the binding site (Fig. 1B) (22). The LALA mutation had no measurable impact on the block to transgene expression by rh9C12 (Fig. 1C), indicating that antibody inhibition is not the result of rerouting virus to a noninfectious and FcγR-dependent cell entry pathway.

As we have previously demonstrated that TRIM21 mediates potent postentry neutralization of Ad5 in cells (20, 23, 24), we sought to determine whether TRIM21 is responsible. We produced a further variant of rh9C12 with mutation H433A, which ablates the interaction with TRIM21 (24). Remarkably, H433A almost completely abolished the antibody block to Ad5 transgene expression in the liver (Fig. 1D). Although the TRIM21 binding site is distinct from that of FcγRs, it does overlap with that of the neonatal Fc receptor (FcRn) (Fig. 1B). To ensure that the phenotype we observed is not caused by a shorter serum $t_{1/2}$ as a result of poorer FcRn-mediated recycling, we determined that mouse FcRn binds WT rh9C12 and H433A with similar efficiency (SI Appendix, Fig. S1 A and B). Furthermore, no difference in the serum levels of these antibodies was detected 24 h post injection (SI Appendix, Fig. S1C), showing that there has been no alteration in FcRn recycling, in accordance with previous reports (25). We sought to confirm this result genetically by repeating the experiment with WT rh9C12 in Trim21 KO mice. Although overall transduction levels in both strains were comparable (SI Appendix, Fig. S2A), the T21-KO mice given rh9C12 closely phenocopied WT mice given the H433A mutant in liver and spleen (Fig. 1D).

Finally, we sought to determine whether TRIM21 blocks gene delivery in the presence of a polyclonal antibody response. We raised anti-serum against Ad5 and found that, although it did not diminish gene transfer (Fig. 1E), it blocked transgene expression (Fig. 1F). At antibody dilutions sufficiently low to inhibit significantly, the effect was TRIM21-dependent. Western blot analysis revealed that the polyclonal serum contained mainly anti-hexon antibodies, but also anti-fiber and low levels of anti-penton base antibodies (SI Appendix, Fig. S3 A and B), indicating that TRIM21 neutralizes in the presence of antibodies against multiple epitopes. To specifically discern the neutralization activity of anti-fiber antibodies, we assessed gene delivery in the presence of the mouse monoclonal anti-fiber antibody 4D2. Although 4D2 reduced gene delivery (SI Appendix, Fig. S3C), the inhibition was only 10-fold, compared with almost 1,000-fold in the case of the anti-hexon monoclonal 9C12. Moreover, there was no TRIM21 contribution (SI Appendix, Fig. S3C), which is consistent with Ad5 biology, as fiber is shed during Ad5 entry and is therefore not associated with the Ad5 capsid in the cytosol (13, 14, 26). Taken together, these data strongly suggest that TRIM21 is responsible for the highly potent block to adenoviral gene delivery by the antibody component of preexisting immunity. Moreover, our data support previous research demonstrating that, although a natural immune response to adenovirus infection elicits anti-fiber and anti-hexon NAbs, the anti-fiber NAbs are less potent than anti-hexon NAbs (11).

In primates and rodents, Ad5 is taken up by multiple cell types, including Kupffer cells and hepatocytes. As TRIM21 is widely expressed in almost all tissues, it may be contributing to responses in both cell types. Upon initial administration of Ad5, the mononuclear phagocytic system acts to clear virus before it can infect the liver parenchyma (27). We therefore sought to deplete macrophages before Ad5 infection to discriminate TRIM21-dependent neutralization in these cells from neutralization in hepatocytes. To this end, we depleted Kupffer cells with clodronate liposomes before Ad5 administration, using markers Adgre1 and Clec4f to confirm depletion (SI Appendix, Fig. S4A). Clodronate-treated mice also had a reduced response to LPS, confirming functional depletion (SI Appendix, Fig. S4B). As treatment with PBS liposomes also slightly attenuated the inflammatory response while not affecting macrophage levels, we used PBS only as our control in subsequent experiments. Macrophage depletion
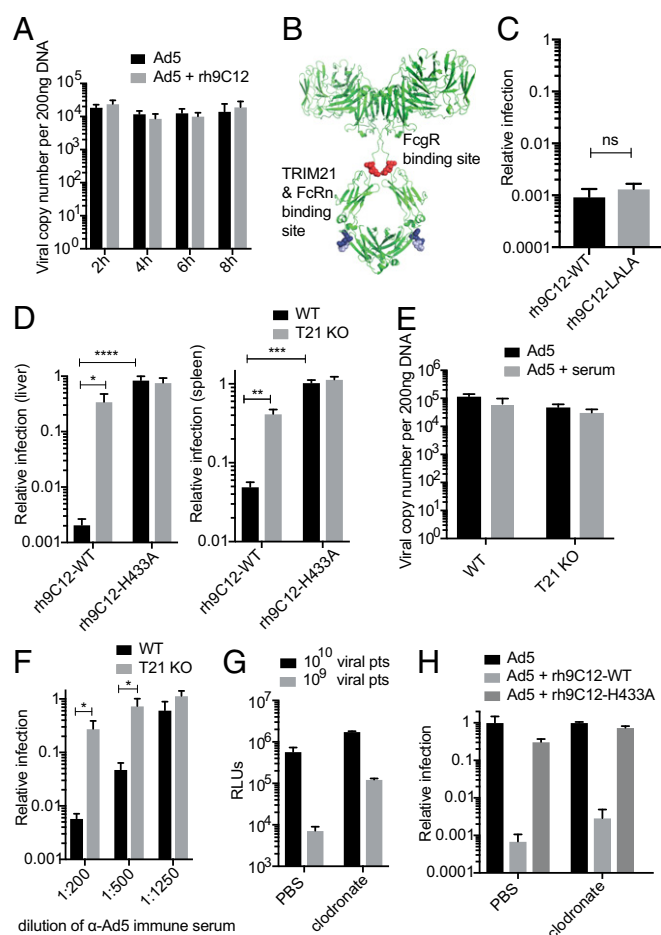

Fig. 1. Diminished transgene expression in the presence of anti-Ad5 antibodies is mediated by TRIM21. (A) Viral copy number at the indicated time points postinfection. (B) Model of human IgG1. Key residues involved in binding to FcγRs are depicted in red (L234/L235), and the TRIM21- and FcRn-binding sites are depicted in blue (H433 in light blue, N434 and H435 in dark blue). (C) Relative infection of Ad5-Luc in mouse liver in WT animals using 2.5 μg WT rh9C12 and FcγR-binding mutant LALA. (D) Relative infection of Ad5-Luc in mouse liver (Left) and spleen (Right) in WT and T21-KO animals using 1 μg WT rh9C12 and TRIM21 nonbinding mutant H433A. (E) Viral copy number 4 h postinfection with anti-Ad5 immune serum (diluted 1:500). (F) Relative infection of Ad5-Luc in mouse liver using the indicated dilutions of anti-Ad5 immune serum in WT and T21-KO animals. (G) Absolute levels of infection measured in relative light units (RLUs) in clodronate-treated or control mice. (H) Relative infection in clodronate-treated or control mice using 1 μg WT rh9C12 and TRIM21 nonbinding mutant H433A. Error bars depict mean ± SEM. Groups consisted of n = 3–10 mice.

48 h before Ad5 infection increased transgene expression (Fig. 1*G*), consistent with their known role in clearing virus and limiting transduction. The greatest impact was seen at a lower viral dose of 10^9, with eightfold higher transgene expression in clodronate-treated animals. This is consistent with macrophages preferentially taking up virus but becoming saturated at a high viral dose, allowing productive transduction of hepatocytes. This finding is in agreement with previous reports of a nonlinear dose–response relation in mice given sequential doses of Ad5, whereby the first dose was shown to saturate Kupffer cells, allowing more virions in the second dose to productively infect hepatocytes (28). When mice were infected with Ad5-Luc in the presence of WT rh9C12, transgene expression was strongly reduced in PBS- and clodronate-treated mice (Fig. 1*H*). This reduction was largely TRIM21-dependent in both conditions and suggests that TRIM21 can efficiently block gene delivery in hepatocytes, independent from neutralization in macrophages.

Efficient gene delivery is important in adenovirus-based vaccines, which are used to deliver T cell epitopes and induce a cytotoxic CD8 T cell response. A TRIM21-dependent block to transgene expression might be expected to severely limit CD8 induction, but activation of TRIM21 also results in potent immune stimulation (21), which could have the opposite effect. Therefore, to test the impact of TRIM21 on the induction of cytotoxic T cells (CTLs) by Ad5 vectors, we made use of the ovalbumin antigen-presentation model system. Ovalbumin contains the immunodominant CD8 T cell epitope SIINFEKL (SL8), and anti-SL8 CTLs can be quantified after immunization by using specific MHC class I tetramers. We analyzed the percentage of SL8-specific T cells 10 d after infection with an Ad5 ovalbumin transgene vector (Ad5-Ova). We observed strong induction of SL8-specific T cells in i.v. immunized animals, which was reduced almost two orders of magnitude, to PBS control levels, in the presence of WT rh9C12 (Fig. 2*A*). Importantly, and in contrast to WT antibody, the H433A mutant did not significantly reduce antigen-specific CTL induction. We obtained similar results upon vaccination of T21-KO mice, confirming that TRIM21 represents a significant block to CTL induction (Fig. 2*B*). However, i.v. administration is only one possible immunization route, and it has been shown that intranasal administration of Ad5 can circumvent preexisting immunity in nonhuman primates (29). To test this in our model, we intranasally administered the same viral dose as in i.v. injections (*SI Appendix*, Fig. S5*A*). We observed markedly reduced induction of SL8-specific CD8 T cells compared with i.v. administration of Ad5-Ova, but no inhibition by rh9C12-WT.

Influenza causes seasonal epidemics and is a key focus of vaccine efforts. We therefore investigated whether TRIM21 would significantly inhibit an i.v.-administered adenovirus-based vector designed to vaccinate against flu infection. We constructed a variant of the influenza virus A/Puerto Rico/8/1934/ (H1N1) strain in which the SL8 peptide (ovalbumin residues 257–264) was incorporated into the stalk of the viral neuraminidase protein (PR8-SL8). Next, we immunized mice i.v. with the Ad5-Ova vector and, 10 d later, administered PR8-SL8 intranasally. Three days after flu infection, we measured viral replication in the lungs by qPCR. Animals that had been vaccinated with Ad5-Ova had a significantly lower viral burden compared with those in the control nonvaccinated group (Fig. 2*C*). Animals that had been vaccinated with Ad5-Ova in the presence of WT rh9C12 had similar levels of flu in their lungs as nonvaccinated controls, demonstrating that the antibody had ablated any benefit from vaccination. By comparison, the H433A mutant did not prevent effective Ad5-Ova vaccination, as these animals were able to reduce flu levels similarly to animals given Ad5-Ova alone.

As the overall reductions in PR8 viral titer achieved by immunization were modest, we established a second model system in which to investigate the TRIM21 block to Ad5 vaccination. We immunized WT or T21-KO animals with Ad5-Ova alone and in the presence of rh9C12-WT or H433A mutant. Seven days later, animals underwent skin graft with the fibrosarcoma tumor
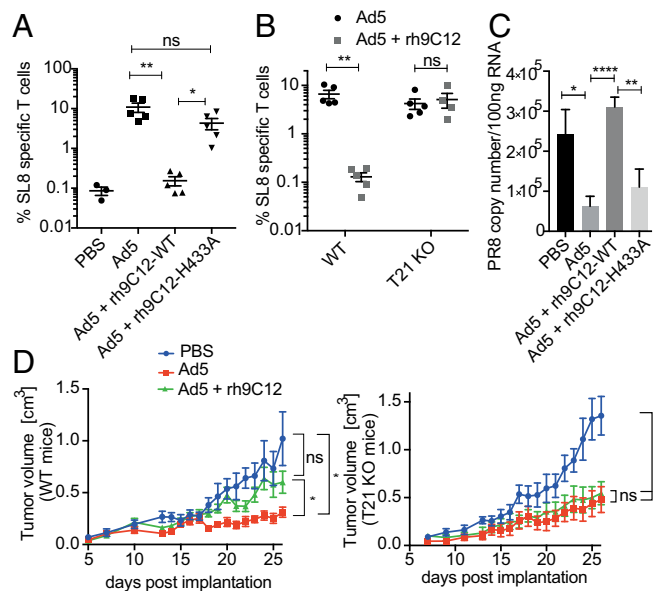

Fig. 2. TRIM21 blocks antigen-specific CD8 T cell responses in an antibody-dependent manner. (*A*) SIINFEKL (SL8)-specific CD8 T cell frequency in the blood of mice i.v. immunized with Ad5-Ova [10^8 particles (pts)] in the presence of WT rh9C12 or H433A. (*B*) SIINFEKL (SL8)-specific CD8 T cell frequency in the blood of WT and T21-KO mice immunized with Ad5-Ova in the presence of WT rh9C12. Error bars depict mean ± SEM. Groups consisted of $n = 4–5$ mice. (*C*) Mice were immunized with Ad5-Ova with or without WT rh9C12 or H433A and infected with PR8-SL8 on day 10 post immunization. Viral titer in the lung was determined 3 d postinfection by qPCR. Error bars depict mean ± SEM. Groups consisted of $n = 5–6$ mice. (*D*) WT (*Left*) or T21-KO (*Right*) animals were immunized with Ad5-Ova only or in the presence of WT rh9C12 and injected with MCA-ovalbumin tumor cells on day 7 post immunization. Error bars depict mean ± SEM. Groups consisted of $n = 5–8$ mice. Tumor growth curves were analyzed by comparing area under the curve by one-way ANOVA with a Tukey post hoc test.

cell line MCA101 secreting ovalbumin (30, 31). Growth of the tumor was monitored regularly by calculating the increase in volume. Rapid tumor growth was observed in nonimmunized animals, with a nonsignificant difference between genotypes. Animals that had been vaccinated with Ad5-Ova displayed significantly reduced tumor growth; however, in WT mice vaccinated with Ad5-Ova in the presence of WT rh9C12, there was only a mild and nonsignificant reduction in tumor growth compared with nonimmunized animals (Fig. 2*D*). This is consistent with a potent antibody block to Ad5-Ova vaccination. Importantly, T21-KO mice immunized with Ad5-Ova in the presence of WT rh9C12 were able to control tumor growth as effectively as those immunized with virus alone. Therefore, TRIM21 antagonizes effective adenovirus vaccination in the context of antiviral and antitumor immunity.

Although the major problem of preexisting immunity to Ad5 is the block to transgene expression, a second problem is that it can elicit an immune response upon vector administration. Studies of the signaling response to Ad5 vectors in the context of preexisting immunity report varying responses depending on what cell type or tissue was analyzed (6, 32, 33). To determine the impact of Ad5 antibody on immune signaling during gene delivery in our experiments, we measured the transcriptional changes in a panel of cytokines, NF-κB target genes, and IFN-stimulated genes (ISGs). We quantified transcriptional changes in the liver at a range of time points postinfection (Fig. 3*A*). Overall, the data show that, at 2, 4, 6, and 8 h after i.v. Ad5 administration, cytokine induction in the presence of antibody is considerably stronger, indicating that antibody promotes an inflammatory response. Although the induction of NF-κB target genes and type I IFN was already observed at 2 h postinfection, the ISGs
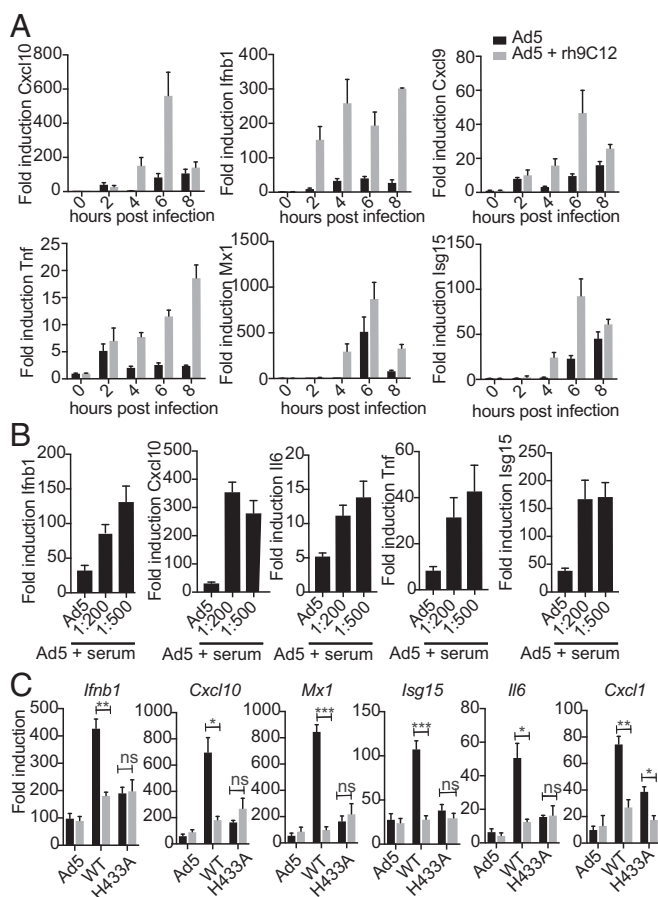
Fig. 3. Anti-Ad5 antibodies elicit a potent inflammatory response. (*A*) Fold induction of cytokines in mouse liver at the indicated time points in response to Ad5 alone (2 × 10^10 pts) or Ad5 and WT rh9C12. (*B*) Fold induction of the indicated cytokines in response to Ad5 alone or and Ad5 and anti-Ad5 immune serum 4 h postinfection. (*C*) Fold induction of the indicated cytokines in the liver of WT (black bars) and T21-KO (gray bars) mice 4 h postinfection. Error bars depict mean ± SEM. Groups consisted of n = 3–5 mice.

Mx1 and *Isg15* were up-regulated only from 4 h postinfection. We obtained similar data by using polyclonal anti-Ad5 sera, confirming that the signaling response was independent of epitope specificity (Fig. 3*B*). Importantly, the transcriptional changes evoked by virus and antibody were of similar magnitude as those induced 4 h after challenge with the TLR7 agonist resiquimod or TLR9 agonist CpG (*SI Appendix*, Fig. S6*A*). These results underline the biological significance of the signaling response to Ad5 induced by antibody. Moreover, use of the H433A mutant or T21-KO mice demonstrated that TRIM21 contributes to the antibody stimulation of immune signaling (Fig. 3*C*). In five of the six genes analyzed, we observed no additive effect of H433A and *Trim21* KO, indicating that TRIM21's role in immune signaling is solely antibody-dependent.

To further investigate the role of TRIM21 in activating immunity and determine the exact nature of the transcriptional program that TRIM21 mediates upon infection, we analyzed genome-wide differential gene expression by RNA sequencing (RNA-seq). First, we determined whether TRIM21 requires antibody to alter transcription during infection. Strikingly, we found that, in uninfected animals or animals infected with Ad5 alone, KO of *Trim21* had minimal impact on gene expression, whereas infection in the presence of rh9C12-WT resulted in almost 700 differentially expressed genes between the genotypes (Fig. 4*A*). Comparison of WT and T21-KO mice infected in the presence of rh9C12-H433A revealed only nine differentially

expressed genes, supporting the previous observation of no additive effect of H433A and *Trim21* KO (*SI Appendix*, Fig. S6*B*). Thus, TRIM21 does not possess gene-regulatory activity during infection outside of its function as an antibody receptor. This is a key finding given that nonantibody-dependent immune functions have been proposed for TRIM21, specifically negative regulatory roles through interaction with IRF3 (34), IRF7 (35), and DDX41 (36).

To determine the specific contribution TRIM21 makes to immune signaling during viral challenge, we analyzed the total transcriptional changes induced by Ad5 infection. We found 995 differentially expressed genes [false discovery rate (FDR)-adjusted *P* < 0.05] between uninfected and infected WT mice, with 574 being up-regulated and 421 being down-regulated. A total of 31.9% of these genes could be classified as immune genes (Fig. 4*B* and Dataset S1) and were largely up-regulated. Within these immune genes, the most up-regulated group consisted of acute phase proteins, such as C-reactive protein and the serum amyloid A family. Furthermore, there was a strong innate immune response, with intrinsic immunity, innate immune signaling, and innate immune sensors constituting 32.8% of the overall immune response.

Next, we investigated how the antiviral immune response is altered in the presence of antibody (Fig. 4*C*). We isolated all significantly differentially expressed genes (FDR-adjusted *P* < 0.05) between WT mice infected with Ad5 alone or in the presence of rh9C12-WT and focused on immune annotated genes [based on Gene Ontology (GO) term: immune system process, GO:0002376]. Infection in the presence of WT rh9C12 induced the strongest response in this group, as indicated by the largest row Z-scores, with the majority of genes being expressed at the highest level in this condition. Notably, several genes that were strongly antibody-induced when measured by qPCR, such as *Cxcl10*, *Mx1*, *Cxcl1*, and *Isg15* (Fig. 3*C*), were among those most highly expressed upon stimulation with Ad5 and rh9C12-WT in this transcriptome-wide analysis. The data suggest that a component of antibody dependent stimulation is TRIM21-mediated, as the expression of this immune gene set between virus only and virus + rh9C12-H433A was more similar than between virus + rh9C12-WT and virus + rh9C12-H433A. However, although the row Z-scores reveal a trend of transcriptional changes suggestive of immune up-regulation by TRIM21, they do not imply statistical significance. To determine whether the changes in gene expression induced by TRIM21 are statistically significant, we analyzed the TRIM21-dependent differential gene expression (FDR-adjusted *P* < 0.05). We employed two different comparisons to determine the TRIM21-dependent transcriptional changes and compared differential gene expression between Ad5 + rh9C12-WT in WT and T21-KO animals as well as between Ad5 + rh9C12-WT and Ad5 + rh9C12-H433A in WT animals (Fig. 4*D*). In each group, we found more than 600 genes that were statistically significantly differentially expressed (984 genes in total), of which 416 occurred in both comparisons. Thus, there is a consistent statistically significant effect when perturbing TRIM21 function genetically or at the level of protein–protein interaction with antibody.

The TRIM21-dependent transcriptional changes demonstrate its role as a positive immune regulator. Detailed analysis revealed that 43.9% of the differentially regulated genes could be classified as immune genes (Fig. 4*D* and Dataset S2), whereas the remaining 56.1% consisted of genes related to common cellular processes. The vast majority of genes influenced by TRIM21 were up-regulated. Crucially, the only genes down-regulated by TRIM21 were involved in metabolism. Focusing on the immune genes, we found that TRIM21 initiated a strong innate immune response, with intrinsic immunity, innate immune signaling, and innate immune sensors accounting for 49.8% of the up-regulated immune genes. Importantly, the pattern of TRIM21-dependent gene expression was different from that induced by virus only (Fig. 4 *B* and *D*). This indicates that TRIM21 does not amplify all transcriptional changes induced
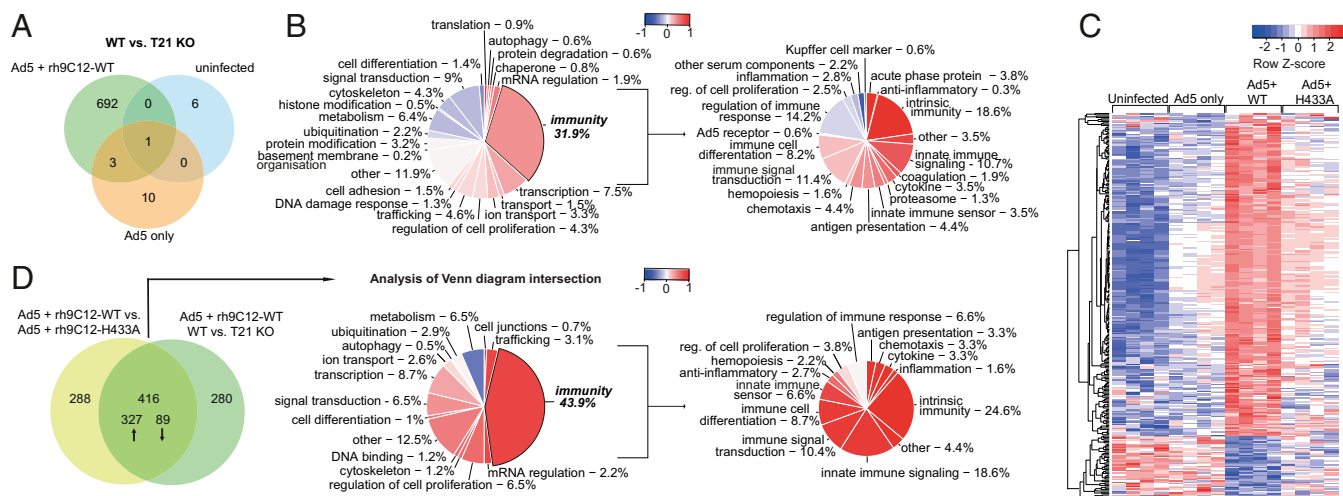
Fig. 4. TRIM21 positively regulates innate immunity in response to Ad5 infection in the presence of antibody. (*A*) Venn diagram comparing differential gene expression between WT and T21-KO animals in uninfected mice, mice infected with Ad5 (2×10^{10} pts), and mice infected with Ad5 in the presence of rh9C12-WT. The gene common to all groups (i.e., intersection of the Venn diagram) is *Trim21*. (*B*) Classification of 995 differentially expressed genes upon virus infection in WT mice. Pie chart colors correspond to the relative number of up- and down-regulated genes separately for each classification according to (genes^{up} − genes^{down})/genes^{total}. (*C*) Heat map of differentially expressed immune genes (GO:0002376) between WT mice infected with Ad5 and WT mice infected with Ad5 + rh9C12 WT. Row Z-scores were calculated from rlog-transformed read counts for the conditions shown (*n* = 4 each). Row Z-scores for WT mice in the following conditions are shown: uninfected, Ad5 alone, Ad5 + rh9C12-WT, and Ad5 + rh9C12-H433A. (*D*) TRIM21-dependent differential gene expression. Venn diagram comparing differential gene expression between WT mice infected with Ad5 and rh9C12-WT or rh9C12-H433A and between WT and T21-KO mice infected with Ad5 and rh9C12-WT (*Top*), and classification of the 416 TRIM21-dependent differentially expressed genes (*Bottom Left*), as well as the classification of the 183 immunity genes (*Bottom Right*). Pie chart colors as in *B*. Pie chart classifications: category "immunity" was based on GO term "immune system process" (GO:0002376), whereas all other categories were assigned based on UniProt descriptions of the relevant gene.

by virus alone, but rather that it fine-tunes the immune response and focuses it toward a more innate response. This may reflect that TRIM21 is a component of intrinsic rather than cellular immunity.

Discussion

Adenovirus is an attractive vector for gene therapy and vaccination, but preexisting immunity provides a major obstacle to its widespread use. This is because of the high prevalence of preexisting immunity in the population, which dramatically reduces transgene expression. It has been unclear exactly how antibodies block Ad5 transduction, as they do not block uptake of vector into cells of diverse tissues (6). Here we show that anti-Ad5 antibodies block transgene expression via the intracellular Fc receptor TRIM21. Cytosolic neutralization by TRIM21 explains the previous discrepancy between genome uptake and transgene expression. Furthermore, we show that TRIM21 inhibits the induction of antigen-specific CTLs, which prevents model Ad5 vaccines from inducing protective downstream antiviral and antitumor immunity. This is an interesting finding given that, while TRIM21 reduces transgene expression, it simultaneously boosts immune signaling, which might stimulate a CD8 T cell response. A potential aspect of TRIM21 function we have not investigated here is whether TRIM21 could contribute to the induction of a CD8 T cell response against structural proteins of the vector. It has previously been shown that cellular immunity does not require de novo translation of viral proteins (37), and because TRIM21 action results in rapid and specific proteasomal degradation of the viral capsid, this could facilitate TAP-mediated transfer of peptides into the endoplasmic reticulum and therefore enhance MHC class I presentation of vector antigens.

A further potential problem caused by preexisting immunity during Ad5 gene therapy is the induction of a transgene-independent immune response (38). There are conflicting reports, which vary from observing increased serum cytokine levels (6, 32), strong liver toxicity (39), and even animal death (32) in the presence of anti-Ad5 antibodies to decreased toxicity (40) and attenuated cytokine induction in peripheral blood

mononuclear cells (33). Our data show that, after i.v. administration of Ad5, immune signaling is strongly induced in the presence of anti-Ad5 antibody and that a significant part of this signaling is TRIM21-dependent. We found that, although not up-regulating a unique set of genes, TRIM21 fine-tunes the immune response already evoked by virus alone and focuses it toward a stronger innate and intrinsic immune response. Gene therapy clinical trials suggest that the problem of preexisting immunity can be circumvented through a lower viral dose and local administration (41, 42). Consistent with this, we observed a reduced block to CD8 cell induction by antibodies and TRIM21 when vector was given intranasally. However, under naïve conditions, T cell induction upon intranasal administration was ~10-fold weaker than via the i.v. route, suggesting that it may be more beneficial to block preexisting immunity than alter delivery regimen. The identification of TRIM21 as a major player in the preexisting immune block to adenovirus gene therapy highlights the importance of understanding how this cytosolic protein is activated and regulated. In doing so, we can hope to augment its activity when advantageous or disrupt it when beneficial.

Materials and Methods

Animal Procedures. All animal work was licensed under the UK Animals (Scientific Procedures) Act 1986 and approved, together with human cell work, by the Medical Research Council Animal Welfare and Ethical Review Body. C57BL/6 WT (T21$^{+/+}$) and TRIM21-deficient mice (T21$^{−/−}$) were obtained from Jackson Laboratories. Ad5 injections at the indicated dose were administered in 100 μL endotoxin-free PBS by lateral tail vein injection (i.v.) or in 20 μL by intranasal administration. PR8 infections were by intranasal administration of 10^3 pfu PR8-SL8 in 20 μL endotoxin-free PBS (Teknova) 10 d after immunization with Ad5-Ova. Details of PR8-SL8 are provided in *SI Appendix, Supplementary Materials and Methods*. For challenge with TLR agonists, mice were injected with 50 μg of resiquimod (R848; Invivogen) and 50 μg CpG (ODN 2395; Invivogen) in 100 μL endotoxin-free water and culled 4 h post injection.

Ex Vivo Viral Assays. Relative infection was calculated from the luciferase signal from indicated tissues (RLUs virus+antibody/RLUs virus only). Transcriptional changes were determined by qPCR. T cell assays were carried out

on specific CD8a cells by H-2K[b]-SIINFEKL tetramer staining. Further details are provided in *SI Appendix, Supplementary Materials and Methods*.

Tumor Growth Experiments. A total of 2.5×10^5 MCA101 cells stably transfected with a plasmid encoding secreted ovalbumin (provided by Clotilde Théry, Institut Curie, PSL Research University, INSERM U932, Paris) were injected s.c. into mice, and tumor growth was monitored by regular volume measurement: $(length*width^2)/2$.

Liver Macrophage Depletion. Mice were given 100 μL of clodronate liposomes (Liposoma) or PBS control by i.v. Virus or LPS (420 μg per mouse) was given 48 h after liposome injection.

Elisa. Hexon and FcRn binding was determined by capture on coated plates (Bio-Rad) and serum levels of rh9C12 by anti-Fc plates (Southern Biotech). Full details are provided in *SI Appendix, Supplementary Materials and Methods*.

Surface Plasmon Resonance. Surface plasmon resonance was performed by using a BIAcore T200 instrument (GE Healthcare). The Langmuir 1:1 ligand-binding model provided by the BIAevaluation software was used to determine binding kinetics. Full details are provided in *SI Appendix, Supplementary Materials and Methods*.

RNA-Seq. RNA-seq library preparation was performed by using the TruSeq stranded mRNA Library Prep kit (Illumina) according to the manufacturer's instructions. A minimum of 20 million reads (SE50) was obtained per sample on a HiSeq 4000 system (Illumina). Sequencing as well as sequence demultiplexing of samples according to barcodes was performed at the CRUK Genomics Core, Cambridge, United Kingdom. Further details are provided in *SI Appendix, Supplementary Materials and Methods*.

Statistical Analysis. Unless otherwise indicated, statistical analyses were performed by using GraphPad Prism 7 software (GraphPad). Error bars depict the SD or SEM as indicated. Unless otherwise indicated, statistical significance was calculated by using an unpaired, two-tailed Student's *t* test. Statistical significance is depicted at the levels of $P \leq 0.05$, $P \leq 0.01$, and $P \leq 0.001$.

1. The Journal of Gene Medicine (2017) Vectors used in gene therapy clinical trials, updated November 2017. Available at abedia.com/wiley/vectors.php. Accessed November 15, 2017.
2. Crystal RG (2014) Adenovirus: The first effective *in vivo* gene delivery vector. *Hum Gene Ther* 25:3–11.
3. Abbink P, et al. (2007) Comparative seroprevalence and immunogenicity of six rare serotype recombinant adenovirus vaccine vectors from subgroups B and D. *J Virol* 81:4654–4663.
4. Nwanegbo E, et al. (2004) Prevalence of neutralizing antibodies to adenoviral serotypes 5 and 35 in the adult populations of the Gambia, South Africa, and the United States. *Clin Diagn Lab Immunol* 11:351–357.
5. Sumida SM, et al. (2005) Neutralizing antibodies to adenovirus serotype 5 vaccine vectors are directed primarily against the adenovirus hexon protein. *J Immunol* 174:7179–7185.
6. Varnavski AN, et al. (2002) Preexisting immunity to adenovirus in rhesus monkeys fails to prevent vector-induced toxicity. *J Virol* 76:5711–5719.
7. McCoy K, et al. (2007) Effect of preexisting immunity to adenovirus human serotype 5 antigens on the immune responses of nonhuman primates to vaccine regimens based on human- or chimpanzee-derived adenovirus vectors. *J Virol* 81:6594–6604.
8. Pine SO, et al. (2011) Pre-existing adenovirus immunity modifies a complex mixed Th1 and Th2 cytokine response to an Ad5/HIV-1 vaccine candidate in humans. *PLoS One* 6:e18526.
9. Sumida SM, et al. (2004) Neutralizing antibodies and CD8+ T lymphocytes both contribute to immunity to adenovirus serotype 5 vaccine vectors. *J Virol* 78:2666–2673.
10. Youil R, et al. (2002) Hexon gene switch strategy for the generation of chimeric recombinant adenovirus. *Hum Gene Ther* 13:311–320.
11. Bradley RR, Lynch DM, Iampietro MJ, Borducchi EN, Barouch DH (2012) Adenovirus serotype 5 neutralizing antibodies target both hexon and fiber following vaccination and natural infection. *J Virol* 86:625–629.
12. Bradley RR, et al. (2012) Adenovirus serotype 5-specific neutralizing antibodies target multiple hexon hypervariable regions. *J Virol* 86:1267–1272.
13. Luisoni S, et al. (2015) Co-option of membrane wounding enables virus penetration into cells. *Cell Host Microbe* 18:75–85.
14. Burckhardt CJ, et al. (2011) Drifting motions of the adenovirus receptor CAR and immobile integrins initiate virus uncoating and membrane lytic protein exposure. *Cell Host Microbe* 10:105–117.
15. Mallery DL, et al. (2010) Antibodies mediate intracellular immunity through tripartite motif-containing 21 (TRIM21). *Proc Natl Acad Sci USA* 107:19985–19990.
16. Fletcher AJ, Mallery DL, Watkinson RE, Dickson CF, James LC (2015) Sequential ubiquitination and deubiquitination enzymes synchronise the dual sensor and effector functions of TRIM21. *Proc Natl Acad Sci USA* 112:10014–10019.
17. Fletcher AJ, James LC (2016) Coordinated neutralization and immune activation by the cytosolic antibody receptor TRIM21. *J Virol* 90:4856–4859.
18. McEwan WA, et al. (2013) Intracellular antibody-bound pathogens stimulate immune signaling via the Fc receptor TRIM21. *Nat Immunol* 14:327–336.
19. Watkinson RE, McEwan WA, Tam JCH, Vaysburd M, James LC (2015) TRIM21 promotes cGAS and RIG-I sensing of viral genomes during infection by antibody-opsonized virus. *PLoS Pathog* 11:e1005253.
20. Bottermann M, et al. (2016) Antibody-antigen kinetics constrain intracellular humoral immunity. *Sci Rep* 6:37457.
21. Xu Z, Tian J, Smith JS, Byrnes AP (2008) Clearance of adenovirus by Kupffer cells is mediated by scavenger receptors, natural antibodies, and complement. *J Virol* 82:11705–11713.
22. Wines BD, Powell MS, Parren PWHI, Barnes N, Hogarth PM (2000) The IgG Fc contains distinct Fc receptor (FcR) binding sites: The leukocyte receptors Fc gamma RI and Fc gamma RIIa bind to a region in the Fc distinct from that recognized by neonatal FcR and protein A. *J Immunol* 164:5313–5318.
23. Vaysburd M, et al. (2013) Intracellular antibody receptor TRIM21 prevents fatal viral infection. *Proc Natl Acad Sci USA* 110:12397–12401.
24. Foss S, et al. (2016) TRIM21 immune signaling is more sensitive to antibody affinity than its neutralization activity. *J Immunol* 196:3452–3459.
25. Kim JK, et al. (1999) Mapping the site on human IgG for binding of the MHC class I-related receptor, FcRn. *Eur J Immunol* 29:2819–2825.
26. Snijder J, et al. (2013) Integrin and defensin modulate the mechanical properties of adenovirus. *J Virol* 87:2756–2766.
27. Stone D, et al. (2007) Adenovirus-platelet interaction in blood causes virus sequestration to the reticuloendothelial system of the liver. *J Virol* 81:4866–4871.
28. Tao N, et al. (2001) Sequestration of adenoviral vector by Kupffer cells leads to a nonlinear dose response of transduction in liver. *Mol Ther* 3:28–35.
29. Richardson JS, Pillet S, Bello AJ, Kobinger GP (2013) Airway delivery of an adenovirus-based Ebola virus vaccine bypasses existing immunity to homologous adenovirus in nonhuman primates. *J Virol* 87:3668–3677.
30. Zeelenberg IS, et al. (2008) Targeting tumor antigens to secreted membrane vesicles in vivo induces efficient antitumor immune responses. *Cancer Res* 68:1228–1235.
31. Sedlik C, et al. (2014) Different immunogenicity but similar antitumor efficacy of two DNA vaccines coding for an antigen secreted in different membrane vesicle-associated forms. *J Extracell Vesicles* 3:24646.
32. Varnavski AN, Calcedo R, Bove M, Gao G, Wilson JM (2005) Evaluation of toxicity from high-dose systemic administration of recombinant adenovirus vector in vector-naive and pre-immunized mice. *Gene Ther* 12:427–436.
33. Zak DE, et al. (2012) Merck Ad5/HIV induces broad innate immune activation that predicts CD8+ T-cell responses but is attenuated by preexisting Ad5 immunity. *Proc Natl Acad Sci USA* 109:E3503–E3512.
34. Higgs R, et al. (2008) The E3 ubiquitin ligase Ro52 negatively regulates IFN-beta production post-pathogen recognition by polyubiquitin-mediated degradation of IRF3. *J Immunol* 181:1780–1786.
35. Higgs R, et al. (2010) Self protection from anti-viral responses–Ro52 promotes degradation of the transcription factor IRF7 downstream of the viral Toll-Like receptors. *PLoS One* 5:e11776.
36. Zhang Z, et al. (2013) The E3 ubiquitin ligase TRIM21 negatively regulates the innate immune response to intracellular double-stranded DNA. *Nat Immunol* 14:172–178.
37. Kafri T, et al. (1998) Cellular immune response to adenoviral vector infected cells does not require de novo viral gene expression: Implications for gene therapy. *Proc Natl Acad Sci USA* 95:11377–11382.
38. Muruve DA, Barnes MJ, Stillman IE, Libermann TA (1999) Adenoviral gene therapy leads to rapid induction of multiple chemokines and acute neutrophil-dependent hepatic injury in vivo. *Hum Gene Ther* 10:965–976.
39. Vlachaki MT, et al. (2002) Impact of preimmunization on adenoviral vector expression and toxicity in a subcutaneous mouse cancer model. *Mol Ther* 6:342–348.
40. Dhar D, Spencer JF, Toth K, Wold WS (2009) Pre-existing immunity and passive immunity to adenovirus 5 prevents toxicity caused by an oncolytic adenovirus vector in the Syrian hamster model. *Mol Ther* 17:1724–1732.
41. Crystal RG, et al. (2002) Analysis of risk factors for local delivery of low- and intermediate-dose adenovirus gene transfer vectors to individuals with a spectrum of comorbid conditions. *Hum Gene Ther* 13:65–100.
42. Wilson JM (2009) Lessons learned from the gene therapy trial for ornithine transcarbamylase deficiency. *Mol Genet Metab* 96:151–157.